Int. J. Electrochem. Sci., 17 **(2022)** Article Number: 22127, doi: 10.20964/2022.12.07

International Journal of
ELECTROCHEMICAL
SCIENCE
www.electrochemsci.org

Effect of Ni-Coated Multi-Walled Carbon Nanotubes on the Properties of Ni-B Composite Coatings on Aluminium Alloys

Huizhong Ma, Hui Bai, Lan Zhang[*]*, Desen Cheng*

School of Mechanics and Safety Engineering, Zhengzhou University, Zhengzhou, Henan, China, Postcode: 450000
[*]E-mail: lanzzu@163.com

Received: 14 August 2022 / *Accepted:* 9 October 2022 / *Published:* 17 November 2022

In this study, a Ni-B-NiMCNT composite was successfully coated onto the surface of a 7075 aluminium alloy using the electrodeposition technique. To investigate and identify the coating properties, we performed XRD(X-Ray Diffraction), SEM(scanning electron microscopy), EDS(energy-dispersive spectroscopy), microhardness testing, and friction wear testing. We discovered that the grain size of the plated layer decreases after the addition of NiMCNT. Also, the uniform distribution of Ni-coated MCNT fills the cracks and gaps in the hydrogen precipitation process and alters the coating morphology. These properties offer the composite coating and substrate interface a strong bonding force. Additionally, NiMCNT causes the growth of small nodules by inhibiting grain growth. An excellent composite layer can be obtained at a current density of 2.5 A/dm^2, temperature of 45 ℃, rotational speed of 350 r/min, and NiMCNT concentration of 0.6 g/L. The hardness of the composite coating is 1265.4 HV, which is 41.2% higher than that of the Ni-B coating. Also, the minimum average friction coefficient is 0.4857, which is 16.6% lower than the Ni-B coating. We employed electrochemical methods to investigate the corrosion resistance of Ni-B-NiMCNT composite plating in 3.5 wt.% NaCl solution. Results indicated that the corrosion resistance of the plate is enhanced when the concentration of NiMCNT in the plating solution is 0.2 g/L.

Keywords: composite electrodeposition, Ni-coated multi-walled carbon nanotubes (NiMCNT), Ni-B composite coating, micromorphology, corrosion resistance

1. INTRODUCTION

Aluminium (Al) and aluminium alloys are versatile materials with tremendous potential for various applications because of their excellent thermal properties, electrical conductivity, light weight, and corrosion resistance [1]. In recent years, Ni-B alloy plating has been utilized in a broad range of applications in the aerospace, automotive, petroleum, plastic, and textile industries due to its outstanding properties such as excellent wear resistance, hardness, corrosion resistance, and thermal stability. As a

result, it is a potential candidate to replace hard chromium plating [2]. Surface mechanical forces cause wear, while environmental electrochemical reactions result in corrosion on the surface of mechanical parts. The combined effect of these two phenomena can lead to severe damage, such as rapid deterioration and failure of mechanical components, which may cause economic losses and even endanger human lives [3]. Producing composite coatings through electrodeposition has recently attracted widespread attention due to its inherent advantages, which include simple processing, easy preparation, low cost, high productivity, and superior synthetic properties [4, 5].

Compared to Ni-P coatings, Ni-B coatings have certain limitations and weaknesses, such as lower corrosion resistance. In genuine industrial environments, corrosion and wear occur simultaneously. Therefore, it is crucial to improve the properties of binary Ni-B coatings so that they can be used in harsher climates and provide greater protection against corrosion and wear [6]. Single-walled and multi-walled carbon nanotubes (CNTs) are particles with outstanding chemical stability and mechanical properties that are used as reinforcing materials. Therefore, CNTs are one of the most popular reinforcing materials, especially for composite coatings [1, 7]. Carbon nanotubes and coaxially nested multi-walled CNTs are hollow tubular bodies formed from seamlessly coiled graphite sheet layers. Compared to steel, CNTs are about 100 times stronger but only one-sixth as dense. They have superior flexibility as well as good chemical stability and a low friction factor [8]. However, the enormous surface energy and high curvature of CNTs prevent the infiltration of most conventional materials. Specifically, CNTs are not uniformly dispersed in the metal matrix and are easily agglomerated. Thus, the bonding between the interface of the carbon nanotubes and the metal matrix is unsatisfactory.

In contrast, Ni-coated multi-walled carbon nanotubes (NiMCNT) are coated with a uniform layer of nickel plating on top of the carbon nanotubes, and there is a bonding between nickel plating. Carbon nanotubes bond better with Ni-coated carbon nanotubes and other metal matrix materials when compounded. Besides, the wettability between the carbon nanotubes and the metal matrix is improved and the dispersion of carbon nanotubes is also enhanced [9-11].

Dong Hongyu deposited carbon nanotubes with different concentrations on the surface of a magnesium alloy matrix with electropulse electrodeposition technology and obtained Ni-GO-CNT composite coatings with self-lubricating properties [12]. Also, Khazeni reported that CNT-enhanced composite coatings had superior mechanical properties to alloy coatings [13]. Prasannakumar investigated Ni-MWCNTs composite coatings for corrosion resistance properties and extended the service life of the coatings [14]. Besides, Sun manufactured Ni-P/CNT composite coatings with excellent mechanical properties by adjusting the pH value [15]. Carpenter investigated the increase in hardness of composite coatings by considering the grain refinement relationship of CNTs distributed in the Ni coating [16]. Ning successfully prepared a copper-carbon nanotube composite coating with higher content and a more uniform distribution of carbon nanotubes. Moreover, the wear rate was 85.4% lower than that of the pure copper matrix [17].

Because aluminium alloys rapidly generate oxide films in an air atmosphere, it is much more challenging to plate composite coatings on this substrate material than on steel sheets. Besides, a more delicate pre-treatment method is required and the selection of a plating solution and its amount is also critical. The main salt of the plating solution used in our experiment was nickel sulfamate, which has

superior properties to the traditional watt's nickel bath, such as a fast deposition rate, strong dispersion ability, and low internal stress of the plated layer. Therefore, nickel sulfamate is more suitable for thick nickel plating. In this study, the Ni-B-NiMCNT coating was prepared by electrodeposition onto a 7075 aluminium alloy. The effect of NiMCNT content on the mechanical properties and microscopic morphology of the composite layer was investigated and the optimum NiMCNT range was determined.

2. EXPERIMENTAL MATERIALS AND METHODS

2.1. Experimental Substrate Material and Treatment

A 7075 aluminium alloy of dimensions 25 mm × 25 mm × 3 mm was used as the substrate material. It was first polished with 240, 600, and 1000 grit SiC papers to obtain a smooth surface. Next, the oil and oxides on the surface were removed by alkaline washing and acid washing in turn.

Aluminium pre-treatment process: Sandblasting → detergent cleaning → degreasing in 3% NaOH alkaline solution for 1 minute → deionised water rinse → ultrasonic cleaning → activation in 3% HCl acid solution for 1 minute → deionised water rinse → ultrasonic cleaning.

2.2 Treatment of NiMCNT

Experimental Ni-coated multi-walled carbon nanotubes with a 30-80 nm outside diameter and a length below 10 μm were purchased from Zhongke Times Nano Company. To further improve the dispersion of the carbon nanotubes, a wet grinding ball milling method was used to pre-treat the carbon nanotubes. First, an appropriate amount of nickel-plated multi-walled carbon nanotubes were weighed, and the mass ratio of steel balls to NiMCNTs was 50:1. The steel balls and the NiMCNTs were submerged in an appropriate amount of alcohol and then ball-milling was performed on a planetary ball mill for 6 h at a speed of 300 r/min with a 5-minute pause every half hour to prevent heat build-up. After ball-milling, the NiMCNT was placed into a drying oven and dried for use. To further improve the dispersibility of the NiMCNTs, mechanical stirring was performed for 0.5 h and ultrasonic dispersion was carried out for a further 0.5 h before the experiment [18]. Figure 1 shows the SEM image of the NiMCNTs before and after ball milling. The ball milling process reduces the length of the NiMCNTs, thereby making them less entangled.

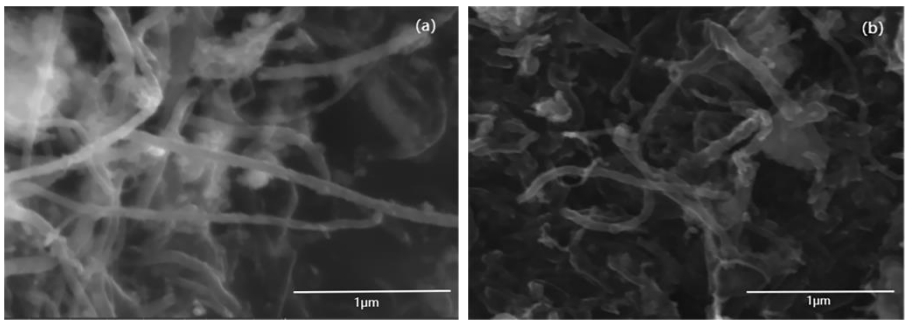

Figure 1. SEM images of (a) pristine NiMCNT powders and (b) ball-milled NiMCNT powders (samples were prepared by electrodepositon at current density 2.5 A/dm^2 for 60 minutes)

2.3. Plating Solution Composition

A 99% purity, 100 mm × 100 mm × 3 mm nickel plate was selected as anode, using nickel sulfamate as the main salt [19]. Trimethylamine borane (TMAB) was then added to the plating solution as a reducing agent and source of boron. The composition of the plating solution and the process parameters are presented in Table 1 and Table 2.

Table 1. Bath composition

Ingredients	Mass concentration (g/L)				
	Ni-B composite coating	Ni-B-NiMCNT-0.2/Ni	Ni-B-NiMCNT-0.4/Ni	Ni-B-NiMCNT-0.6/Ni	Ni-B-NiMCNT-1.0/Ni
$Ni(NH_2SO_3)_2$	350	350	350	350	350
$NiCl_2 \cdot 6H_2O$	20	20	20	20	20
H_3BO_3	40	40	40	40	40
SDS	0.1	0.1	0.1	0.1	0.1
Saccharin	1	1	1	1	1
TMAB	3	3	3	3	3
NiMCNT	/	0.2	0.4	0.6	1.0

Table 2. Operating conditions

Temperature	45 ℃
Agitation rate	350 r/min
Deposition time	60 min
Current density	2.5 A/dm
pH	4

2.4. Characterisation of Ni-B-NiMCNT Composite Plating and Performance Testing

Characterisation of the solid particles and composite coating morphology was performed by scanning electron microscopy (SEM). Besides, an analysis of the elemental composition of the composite coating was conducted using (EDS). The voltage used was 10kV, the current was 0.69 nA, and the magnification was 5,000 times. The surface micromorphology and roughness of the composite plating were assessed using atomic force microscopy (AFM; SPM-9700, Japan) with a measurement range of 20 μm × 20 μm. A digital microhardness tester (HXD-1000TM, Shanghai Taiming Optical Instruments Co., Ltd.) was used for microhardness testing with a load of 100 g and 15 seconds. The average value was taken from five readings at different locations. A rotary friction tester (MS-T3000, Lanzhou Institute of Chemistry, Chinese Academy of Sciences) was used to test the coefficient of friction(COF) with a load of 200 g and a test time of 30 minutes. The grinding balls used were 3 mm

diameter ZrO_2 balls. The electrochemical performance of the composite plating was tested using an electrochemical workstation (CHI660, Shanghai Chenhua Instruments Co., Ltd.). For this test, the working electrode was a Ni-B-NiMCNT composite plate with an area of 1 cm^2 exposed to 3.5 wt.% NaCl solution at room temperature. The potential was ramped from −1.2 V and-1.2 V. Additionally, the auxiliary electrode was platinum and the reference electrode was silver chloride. The EIS scan frequency was 0.1 Hz to 100 kHz, the amplitude was 10 mV, and the scan rate for the polarisation curve was 1 mV/s. The composite coating was characterised using an X-ray diffractometer (XRD, UItima, Japan) under the conditions of Cu Kα radiation (λ = 0.154 nm), an operating voltage of 40 kV, scanning angle of 30°-90°, and scanning speed of 4 °/min. The average crystallite size of the composite coatings were determined by using the Debye-Scherrer formula as presented in the equation below:

$$D = \frac{k\lambda}{\beta \cos\theta}, \qquad (1)$$

where D is the crystallite size (nm), K is the Scherrer constant, taken as 0.89, λ is the X-ray wavelength, β signifies the diffraction peak half-height width, and θ is the diffraction angle.

3. RESULTS AND DISCUSSION

3.1. Microscopic Morphology and Elemental Analysis of the Composite Coating

Figure 2 illustrates the surface morphology SEM image of Ni-B composite coating and Ni-B-NiMCNT composite coating at different NiMCNT concentrations. The surface morphology of the Ni-B plated layer without the addition of NiMCNT, shown in Figure 2a, the surface morphology presents a typical smooth surface of nickel-based coating.[20] These cracks are the result of hydrogen evolution during the Ni-B deposition process, which changes when 0.2 g/L NiMCNT is added. As the NiMCNT concentration increases, the nodules are more pronounced, laterally reflecting the uniform embedding of the NiMCNTs. Regarding particle distribution, most of the NiMCNTs are embedded in the matrix, with a smaller proportion protruding from the coating surface [15, 21]. At this time, raised small particles are observed on the original smooth Ni-B coating surface. However, because the concentration is so low, there are fewer expanded small particles. When the concentration is 0.6 g/L, the distribution is more uniform because the carbon nanotubes fill the gaps and crevices [5]. Besides, there is no agglomeration and the interface bonding force is also strong. When the concentration rises to 1 g/L, the microscopic morphology of the plated layer becomes darker on some surfaces due to the high concentration of NiMCNT clustered on the surface. Additionally, the surface of the plated layer becomes rough due to excessive NiMCNT adsorption on the cathode surface.

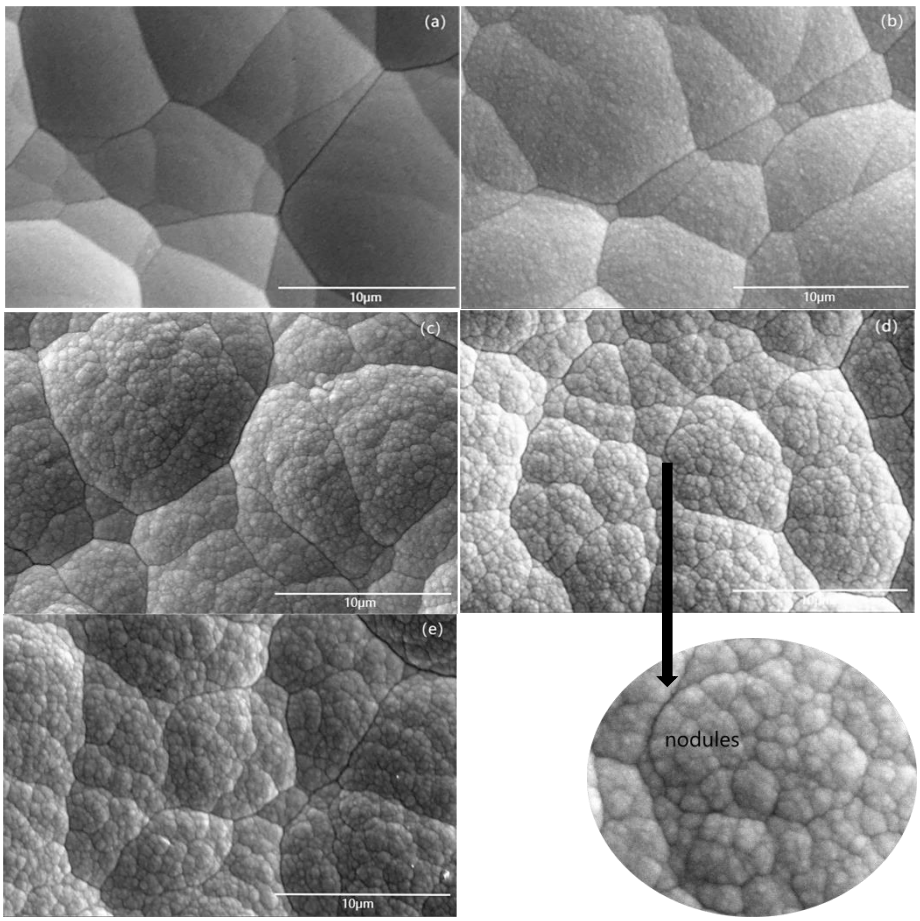

Figure 2. SEM images of (a) Ni-B; (b) Ni-B-NiMCNT-0.2/Ni; (c) Ni-B-NiMCNT-0.4/Ni; (d) Ni-B-NiMCNT-0.6/Ni; (e) Ni-B-NiMCNT-1.0/Ni (samples were prepared by electrodepositon at current density 2.5 A/dm^2 for 60 minutes)

In order to confirm whether NiMCNT is deposited in the Ni-B-NiMCNT composite coating, the chemical composite is analyzed by EDS and shows in Fig. 3. Figure. 4. shows that Ni, B, and NiMCNT were co-deposited in the coating. It reveals that the distribution of elements in the carbon nanotubes co-deposited with Ni-B and the composite coating is relatively uniform without any apparent agglomeration.

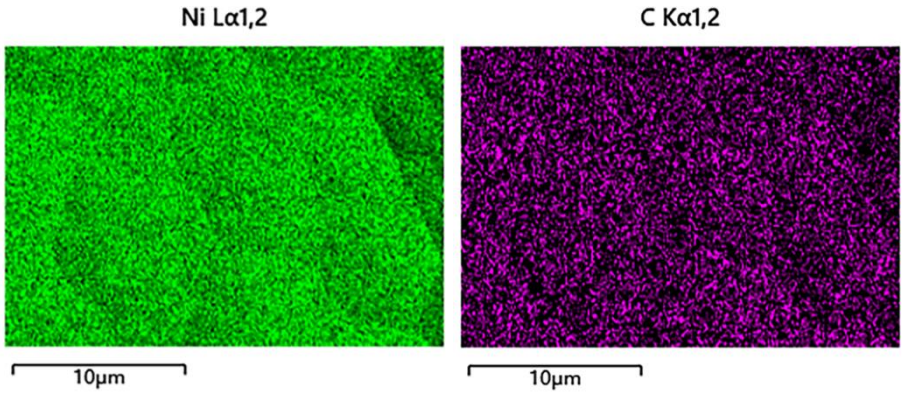

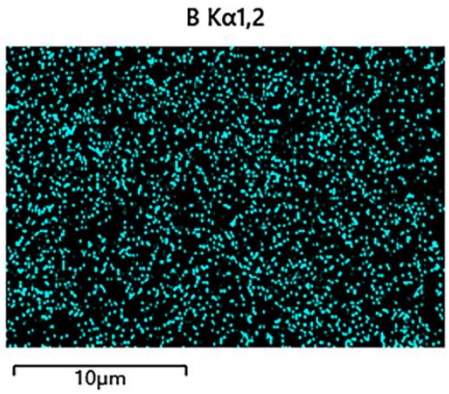

Figure 3. EDS spectra of Ni, C, and B at 0.6 g/L NiMCNT (samples were prepared by electrodepositon at current density 2.5 A/dm^2 for 60 minutes)

AFM is used to study the morphology and roughness of the composite coating on the microscopic scale. Figure 4 shows the AFM diagrams of the composite layer with an observation range of 20 μm × 20 μm. The surface roughness (Ra) is 0.75 μm when the NiMCNT addition is zero. When NiMCNT is added, the surface of the composite layer is hilly, the size of the cellular structure falls, and the morphology of the layer changes significantly. As Table 3 indicates, when 0.6 g/L NiMCNT is added, the roughness (Ra) of the composite coating is 0.36 μm, which is the lowest average roughness value. Compared to Ni-B composite coating roughness decreased by 52 %. The lower surface roughness of the Ni-B-NiMCNT composite coatings is primarily due to the small grains that are uniformly packed together [22, 23].

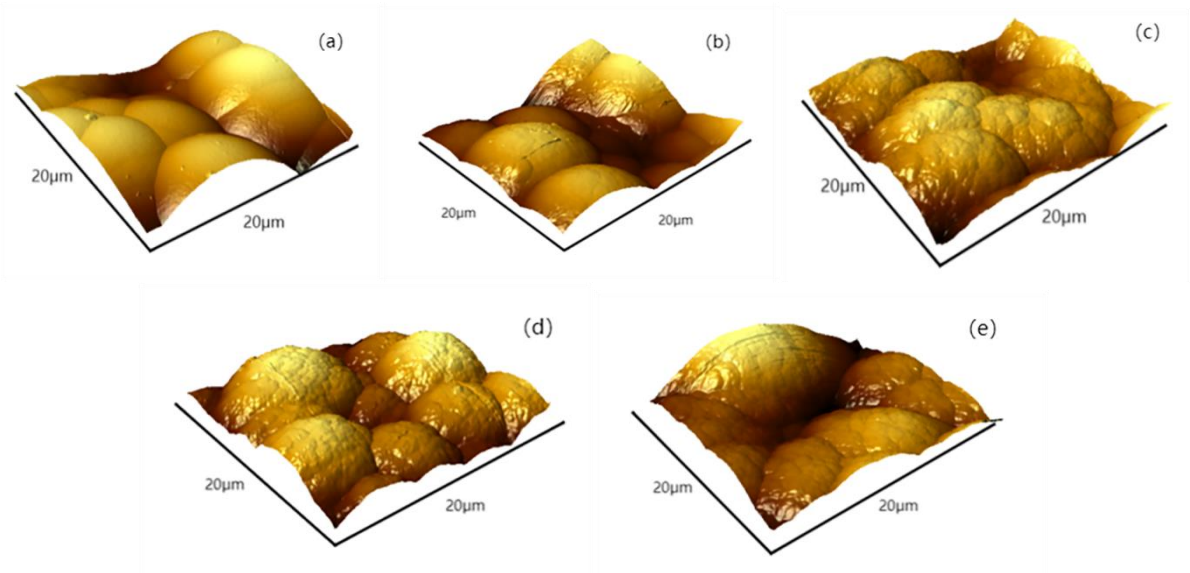

Figure 4. AFM plots of (a) Ni-B; (b) Ni-B-NiMCNT-0.2/Ni; (c) Ni-B-NiMCNT-0.4/Ni; (d) Ni-B-NiMCNT-0.6/Ni; (e) Ni-B-NiMCNT-1.0/Ni (samples were prepared by electrodepositon at current density 2.5 A/dm^2 for 60 minutes)

Table 3. Results of sample AFM surface roughness

Sample	Ra (μm)
Ni-B/Ni	0.75
Ni-B-NiMCNT-0.2/Ni	0.70
Ni-B-NiMCNT-0.4/Ni	0.43
Ni-B-NiMCNT-0.6/Ni	0.36
Ni-B-NiMCNT-1.0/Ni	0.45

3.2 Phase Structure Analysis of the Composite Plating

Figure 5 displays the XRD spectra of the Ni-B composite plating and Ni-B-NiMCNT composite platings with different NiMCNT concentrations. It shows that three characteristic peaks of other crystalline planes appear in the plate at 2θ = 44.5°, 51.8°, and 76.4°, corresponding to the (111), (200), and (220) peaks of Ni, respectively [24]. The C peak was not detected due to the low atomic number of C, while B formed a solid solution with Ni. Also, the peak width of the central peak (111) becomes more pronounced with increasing NiMCNT content, indicating that the addition of NiMCNT reduces the grain size of the plated layer. Similarly, the (200) and (220) peaks decrease as the (111) peak decreases, eventually presenting a relatively low peak. The nickel lattice is distorted, probably due to the addition of NiMCNT, and cannot maintain a face-centred cubic structure, thereby developing towards an amorphous state. Further reasons for this manifestation remain to be studied in detail.

According to Figure 6, the crystal size of the composite coatings at different NiMCNT concentrations shows a trend of first decreasing and then increasing. The grain size reaches a minimum value of 3.819 nm at 0.6 g/L NiMCNT. Compared to the crystal size of 5.612 nm for Ni-B composite coating, the crystal size is reduced by 32 %. This can be explained by the addition of solid particles that prevent the original nickel nucleation. The carbon nanotubes provide more nucleation sites, which retard crystal growth and subsequently result in a smaller crystal size in the corresponding Ni-B matrix of the composite coating [25]. Additionally, when the concentration of NiMCNT is 1 g/L, agglomeration occurs at too high a concentration. This causes the original nickel crystals to grow and results in a slightly increased crystal size.

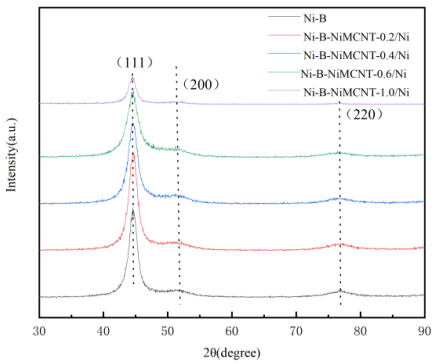

Figure 5. XRD spectra of Ni-B, Ni-B-NiMCNT-0.2/Ni, Ni-B-NiMCNT-0.4/Ni, Ni-B-NiMCNT-0.6/Ni, and Ni-B-NiMCNT-1.0/Ni (samples were prepared by electrodepositon at current density 2.5 A/dm^2 for 60 minutes)

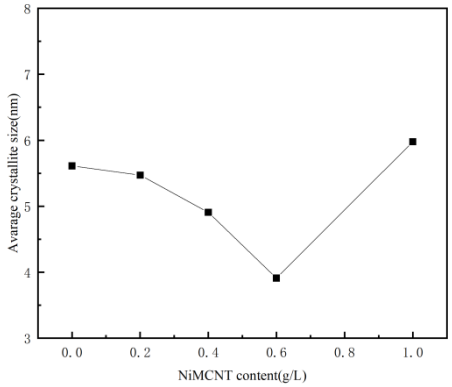

Figure 6. crystal size of Ni-B, Ni-B-NiMCNT-0.2/Ni, Ni-B-NiMCNT-0.4/Ni, Ni-B-NiMCNT-0.6/Ni, and Ni-B-NiMCNT-1.0/Ni (samples were prepared by electrodepositon at current density 2.5 A/dm^2 for 60 minutes)

3.3 Microhardness and Wear Resistance of the Composite Plating

The microhardness of the composite coating as well as the coefficient of friction(COF) are presented in Figure 7. The figure shows that NiMCNT embedding has a considerable strengthening effect on the hardness, and the microhardness of the composite coating exhibits a trend of first increasing and then decreasing. The maximum microhardness of 1265.4 HV is achieved at a NiMCNT concentration of 0.6 g/L, which is 41.2% higher than that of the standard Ni-B coating [20, 26]. The homogeneous dispersion of carbon nanotubes acts as a diffusion reinforcement, which improves the hardness of the composite layer [8, 27]. Moreover, the addition of NiMCNT enhances grain refinement, which also enhances the hardness. When 1 g/L NiMCNT is added, fewer NiMCNTs are embedded in the composite coating due to the agglomeration of NiMCNT, thereby resulting in a decrease in microhardness. Additionally, the COF shows a trend of decreasing and then increasing can be attributed to the self-lubricating property of NiMCNTs.The uniformly dispersed NiMCNTs form an effective lubricant layer, so the coefficient of friction gradually decreases as the NiMCNT concentration increases. When the concentration of NiMCNT is 0.6 g/L, the COF is 0.4857, which is the smallest value and 16.6% lower than the Ni-B coating. When the composite coating is rubbed, one end of the NiMCNTs protrudes from the coating surface and acts as an underprop. However, the other end is still embedded in the composite coating, which prevents the separation of the NiMCNTs from the composite matrix. Owing to their unique self-lubricating ability, NiMCNTs protect the substrate from wear and improve wear resistance [21].

Figure 8 displays the composite plating coefficient of friction diagrams at a load of 200 g and a rotational speed of 200 r/min with 30 minutes of rotational friction. Compared with the Ni-B coating, the COF of the NiMCNT composite coating is substantially lower. The coefficient of friction exhibits more severe fluctuations with the Ni-B coating, probably due to heat generation during wear. This leads to tensile stress at the interface between the amorphous and crystalline phases. Cracking during the

hydrogen evolution reaction also leads to stress concentration, which causes the coating to delaminate and results in fluctuations. As the friction process proceeds from the initial macroscopic wear to diffuse microscopic wear, the NiMCNTs exhibit excellent lubricating properties, as they shear easily and slide into the coating. When 0.2 g/L NiMCNT is added, the COF decreases slightly because the concentration is low and a uniform coating does not form. In contrast, when the concentration of NiMCNT increases to 0.6 g/L, the uniformly dispersed NiMCNTs form a lubricant layer at the friction interface, significantly reducing the COF.

Figure 9 presents the amount of wear for the various Ni-B-NiMCNT composite coatings after 30 minutes of rotational friction under dry friction conditions. The trend for the extent of the wear is similar to that of the COF. More specifically, the wear amount gradually becomes smaller, reaching a minimum at 0.6 g/L NiMCNT with a value of 0.01546 mm^3. Compared to the same conditions Ni-B plating wear amount 0.05278 mm^3 decreased by 70.7%. The low amount of wear and low COF also reflect the superior tribological properties of the plating, and is also related to the high hardness value of the plate and the low roughness of the AFM.

To further investigate the effect of NiMCNT content on the wear resistance of the composite coating, the wear abrasion marks of the coating were tested using SEM, as shown in Figure 10. At zero NiMCNT addition, the wear conditions produce large cracks. The hydrogen precipitation reaction during the electrodeposition of the Ni-B coating results in slight cracks and gaps on the surface. Also, in the vicinity of the abrasion marks, flaking particles appear [28]. This is because when the friction substrate and the plating are in action, the frictional shear force causes particles to fall off the surface of the plate. The peeling particles act as an abrasive material between the friction substrate and the substrate to generate abrasive wear, so the degree of wear is more substantial [25]. Also, when 0.2g/L NiMCNT is added, the cracks become thinner. The diffusion strengthening effect of NiMCNT improves the hardness and strength of the composite coating, thereby resisting wear to the friction substrate and preventing plastic deformation [7].

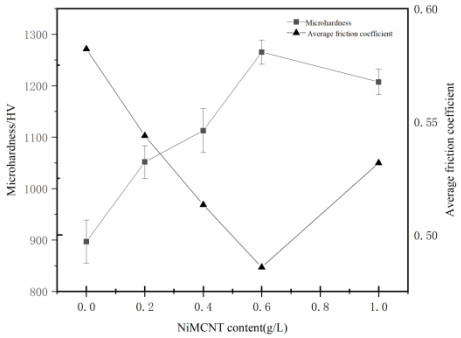

Figure 7. Effect of different NiMCNT additions on Ni-B-NiMCNT composite plating microhardness and average friction coefficient (samples were prepared by electrodepositon at current density 2.5 A/dm^2 for 60 minutes)

However, the NiMCNT does not form an adequate protective coating because the added concentration is too low, so the wear marks are deeper and accompanied by slight cracks. At 0.6 g/L, fine grooves along the sliding direction are observed, indicating that the wear mechanism is abrasive.

Since the NiMCNT cut off by the wear process can be used as a spacer layer to reduce direct contact between the abrasive ball and the coating, it has better wear resistance [18]. At 1 g/L, the abrasion test causes the particles with weak bonding ability to the surface as well as clustered particles to fall off, leading to cracks on the coating surface and a reduction in wear resistance [8].

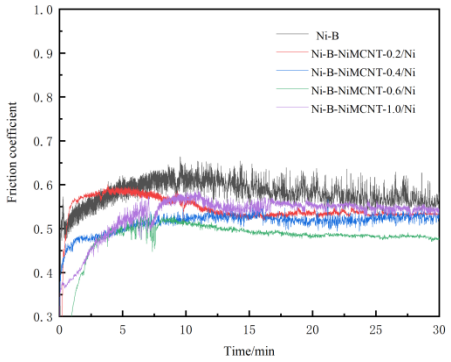

Figure 8. Friction curve of Ni-B-NiMCNT composite coating friction coefficient with time under dry friction conditions (samples were prepared by electrodepositon at current density 2.5 A/dm^2 for 60 minutes)

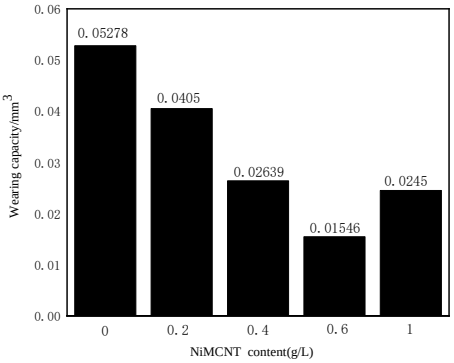

Figure 9. Wear of Ni-B-NiMCNT composite plating under dry friction conditions (samples were prepared by electrodepositon at current density 2.5 A/dm^2 for 60 minutes)

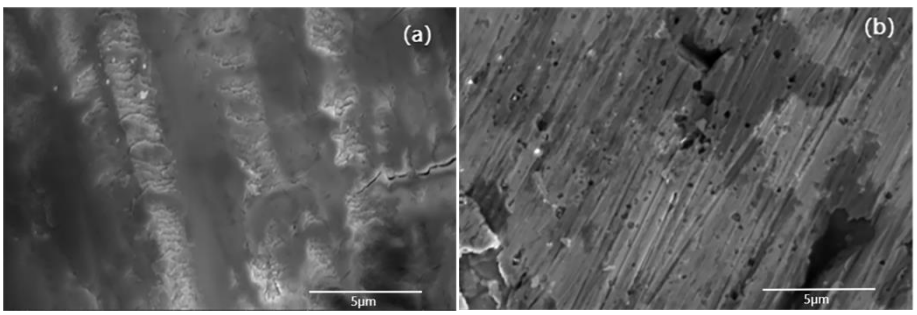

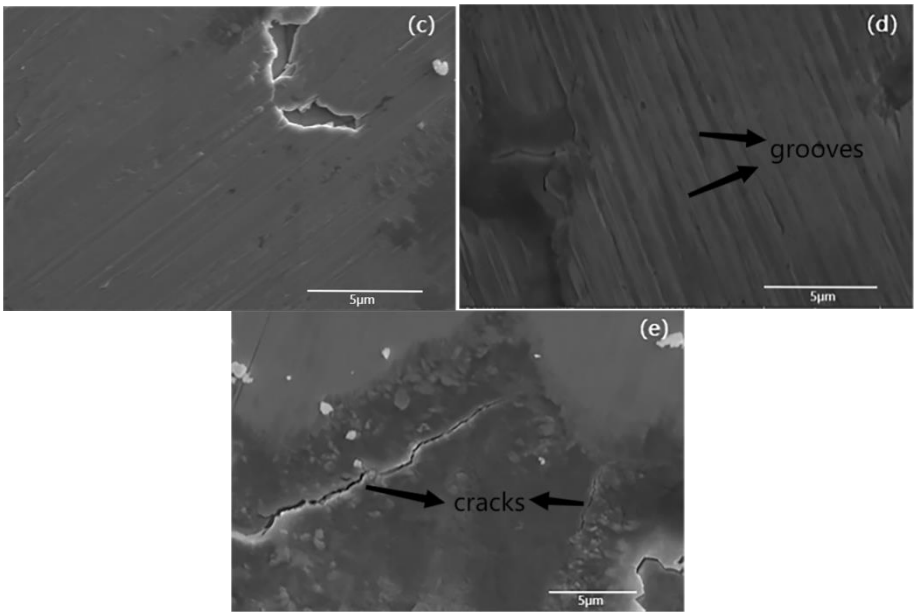

Figure 10. SEM images of Ni-B-NiMCNT composite plating wear marks: (a) Ni-B; (b) Ni-B-NiMCNT-0.2/Ni; (c) Ni-B-NiMCNT-0.4/Ni; (d) Ni-B-NiMCNT-0.6/Ni; (e) Ni-B-NiMCNT-1.0/Ni (samples were prepared by electrodepositon at current density 2.5 A/dm^2 for 60 minutes)

3.4 Corrosion Resistance of the Composite Plating

The AC impedance and potentiodynamic polarization curves of the Ni-B-NiMCNT composite plating with different NiMCNT contents were measured in 3.5 wt.% NaCl solution, and the results are shown in Figure 11. In the Nyquist diagram, the larger the diameter of the semicircular curve of the measured test piece, the higher the resistance value of the test piece, which means the better corrosion resistance of the sample. With an increase in NiMCNT concentration, the capacitive arc radius of the coating decreases, indicating that the corrosion resistance of the composite coatings deteriorates with an increase in CNT concentration. This result is due to the tubular structure of the NiMCNTs, which are carbon-related materials with a nanometer-scale diameter and a perfect hollow molecular structure. NiMCNTs tend to agglomerate, so too many NiMCNTs deposited on the substrate occupy the position of nickel and boron, leading to the accumulation of a large number of carbon nanotubes. This is extremely unfavourable to the coating, resulting in a reduction in corrosion resistance [29]. In the Ni-B coating without NiMCNT addition, the cracks generated by the hydrogen precipitation reaction are considered active sites for corrosion initiation. However, the addition of NiMCNT fills these gaps and cracks and reduces the path of corrosion attack. The fitted impedance data in Table 4 shows that the Rp value of the 0.2 g/L NiMCNT composite coating is 1340 Ω·cm^2, which is superior to the other coatings. Therefore, the dispersion of NiMCNT in the nickel matrix forms numerous corrosion microcells. NiMCNT as the cathode with nickel as the anode accelerates the dissolution of nickel, thus intensifying the corrosion rate. Local corrosion occurs at 1 g/L NiMCNT due to agglomeration, while dislocations also lead to the accumulation of a large amount of surface energy, which also increases the corrosion rate.

The polarization curves in Figure 11b and the fitted data in Table 5 show that the corrosion potential of the composite plating is higher than several other cases at 0.2 g/L NiMCNT concentration, which is consistent with the impedance plots. The fitted data reveal that the corrosion potential of the plating is most positive and the corrosion current is smallest at a concentration of 0.2 g/L NiMCNT. The i_{corr} values of Ni-B composite coating and Ni-B-NiMCNT composite coating deposited on aluminium alloys is 2.23×10^{-5} A/cm2 and 5.04×10^{-5} A/cm2, respectively.With increasing NiMCNT concentrations, the corrosion potential of the composite coating gradually becomes negative, indicating that the corrosion resistance of the composite coating weakens [29]. In general, there is an obvious potential difference between the carbon substrate and the nickel substrate, which is not conducive to improving corrosion resistance [5, 30].

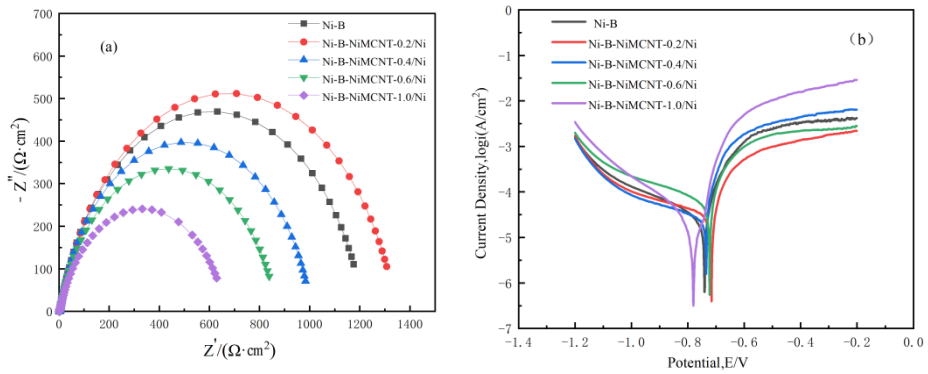

Figure 11. Composite platings with various CNT additions: (a) Impedance spectrum; (b) Potentiodynamic polarisation curves of Ni-B/Ni, Ni-B-NiMCNT-0.2/Ni, Ni-B-NiMCNT-0.4/Ni, Ni-B-NiMCNT-0.6/Ni, Ni-B-NiMCNT-1.0/Ni (samples were prepared by electrodepositon at current density 2.5 A/dm^2 for 60 minutes)

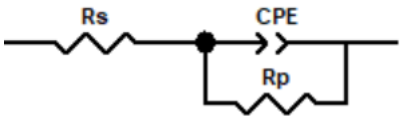

Figure 12. Equivalent circuit diagram of electrochemical corrosion for the composite plating

Table 4. Electrochemical impedance fitting data

	Rs ($\Omega\cdot cm^2$)	Rp ($\Omega\cdot cm^2$)	CPE-T ($\Omega^{-1}\cdot cm^{-2}\cdot s^{-n}$)	CPE-P ($\Omega^{-1}\cdot cm^{-2}\cdot s^{-n}$)
Ni-B/Ni	4.434	1211	1.2195×10^{-4}	0.84031
Ni-B-NiMCNT-0.2/Ni	4.665	1340	9.4155×10^{-5}	0.83143
Ni-B-NiMCNT-0.4/Ni	4.355	1001	11268×10^{-4}	0.85451
Ni-B-NiMCNT-0.6/Ni	4.166	864.3	1.7832×10^{-4}	0.83961
Ni-B-NiMCNT-1.0/Ni	2.866	663	2.5706×10^{-4}	0.7998

Table 5. Corrosion characteristics of the coated samples in 3.5 wt.% NaCl solution

	E_{corr} (V)	I_{corr} (A/cm^2)
Ni-B/Ni	-0.741	2.23×10^{-5}
Ni-B-NiMCNT-0.2/Ni	-0.716	2.32×10^{-5}
Ni-B-NiMCNT-0.4/Ni	-0.735	2.93×10^{-5}
Ni-B-NiMCNT-0.6/Ni	-0.723	5.04×10^{-5}
Ni-B-NiMCNT-1.0/Ni	-0.78	1.98×10^{-5}

4. CONCLUSIONS

(1) A Ni-B-NiMCNT composite layer was obtained through electrodeposition. Results indicate that the addition of NiMCNT effectively improves the mechanical properties of the Ni-B plating. The delicate crystal reinforcement of NiMCNT changes the morphology of the plate and enhances its hardness. Also, the uniformly distributed NiMCNT coating provides the plating stable lubrication and reduces the friction coefficient. The most uniform distribution is achieved with the addition of 0.6 g/L NiMCNT. When the concentration of NiMCNT in the plating solution is 1 g/L, the mechanical properties of the plated layer deteriorate as a result of the weaker bonding with the nickel substrate due to bulging caused by NiMCNT agglomeration.

(2) The corrosion test results show that when 0.2 g/L NiMCNT is added, the corrosion resistance of Ni-B-NiMCNT (Rp = 1340 Ω·cm^2) is optimal because the uniform distribution of NiMCNT fills the crevice cracks and shifts the potential in the positive direction. However, higher concentrations of NiMCNT are not conducive to the improvement of corrosion resistance.

ACKNOWLEDGMENTS
This work was supported by the [Zhongyuan Academacian Fund] under Grant [ZYQR2019120188].

DECLARATION OF INTEREST STATEMENT
The authors report there are no competing interests to declare.

References

1. Z. Zhang, A. Kitada, T. Chen, K. Fukami, M. Shimizu, S. Arai, Z. Yao and K. Murase, *J. Alloy. Compd.,* 816 (2020).
2. E. Unal, A. Yasar and I.H. Karahan, *Mater. Res. Express*., 6 (2019).
3. U.S. Waware, R. Nazir, A. Prasad, A.M.S. Hamouda, A.K. Pradhan, M. Alshehri, R. Syed, A. Malik and M.S. Alqahtan, *Surf. Coat. Technol*., 409 (2021).
4. Z.W. Jia, W.C. Sun, F. Guo, Y.R. Dong and X.J. Liu, *RSC Adv.,* 8 (2018) 12138-12145.
5. A.P. Meshram, M.K.P. Kumar and C. Srivastava, *J. Mater. Eng. Perform*., 31 (2022) 1573-1584.
6. U.S. Waware, A.M.S. Hamouda, B. Bajaj, T. Borkar and A.K. Pradhan, *J. Alloy. Compd*., 769 (2018) 353-359.
7. F. Dogan, E. Duru, M. Uysal, H. Akbulut and S. Aslan, *Jom*., 74 (2022) 574-583.
8. S. Yazdani, R. Tima and F. Mahboubi, *Appl. Surf. Sci.,* 457 (2018) 942-955.
9. X. Zhou, G. Jiang, S. Song, J. Li and L. Liu, *Compos. Interfaces*., 29 (2022) 97-110.

10. M. Qu, Z. Gao, J. Chen and Y. Cui, *J. Mater. Sci-Mater. Electron*., 33 (2022) 10866-10879.
11. M.M. Billah, Q. Chen, *J. Electron. Mater*., 47 (2018) 2366-2373.
12. Y.R. Dong, W.C. Sun, X.J. Liu, Z.W. Jia, F. Guo, M. Ma and Y.Y. Ruan, *Surf. Coat. Technol*., 359 (2019) 141-149.
13. D. Khazeni, M. Saremi and R. Soltani, *Ceram. Int*., 45 (2019) 11174-11185.
14. R.S. Prasannakumar, V.I. Chukwuike, K. Bhakyaraj, S. Mohan and R.C. Barik, *Appl. Surf. Sci.,* 507 (2020).
15. Z. Sun, H. Yang, M. Xiao, Y. Fu, D. Wu and N. Gao, *Arab. J. Sci. Eng*., 45 (2020) 1229-1236.
16. C.R. Carpenter, P.H. Shipway and Y. Zhu, *Surf. Coat. Technol*., 205 (2011) 5059-5063.
17. D. Ning, A. Zhang and H. Wu, *Materials.*, 12 (2019).
18. P. Yang, N. Wang, J. Zhang, Y. Lei and B. Shu, *Mater. Res. Express*., 9 (2022).
19. M. Lekka, R. Offoiach, A. Lanzutti, M.Z. Mughal, M. Sebastiani, E. Bemporad and L. Fedrizzi, *Surf. Coat. Technol*., 344 (2018) 190-196.
20. H.H. Sheu, Q.Y. Wang, P.C. Huang, A.Y. Cheng, Y.M. Liu, K.H. Hou and M.D. Ger, *Int. J. Electrochem. Sci.,* 16 (2021).
21. Z.H. Li, X.Q. Wang, M. Wang, F.F. Wang and H.L. Ge, *Tribol. Int.,* 39 (2006) 953-957.
22. R.A. Shakoor, U.S. Waware, R. Kahraman, A. Popelka and M.M. Yusuf, *Int. J. Electrochem. Sci.,* 12 (2017) 4384-4391.
23. R.A. Shakoor, U.S. Waware, K. Ali, R. Kahraman, A. Popelka, M.M. Yusuf and A. Hasan, *Coatings*., 7 (2017).
24. B. Li, X. Li, Y. Huan, W. Xia and W. Zhang, *J. Alloy. Compd*., 762 (2018) 133-142.
25. L. Shi, C.F. Sun, P. Gao, F. Zhou and W.M. Liu, *Surf. Coat. Technol*., 200 (2006) 4870-4875.
26. A. Mazurek, W. Bartoszek, G. Cieslak, A. Gajewska-Midzialek, D. Oleszak and M. Trzaska, *Arch. Metall. Mater.,* 65 (2020) 839-844.
27. Y. Tao, F. Ma, M. Teng, Z. Jia and Z. Zeng, *Appl. Surf. Sci.,* 492 (2019) 426-434.
28. X. Li, X. Tong, R. Yang, Y. Liu, Q. Wan, L. Mei and J. Wang, *Mater. Rev*., 31 (2017) 66-71.
29. Z. Gao, S. Zhao, Y. Wang, X. Wang and L. Wen, *Int. J. Electrochem. Sci*., 10 (2015) 637-648.
30. C. Guo, Y. Zuo, X. Zhao, J. Zhao and J. Xiong, *Surf. Coat. Technol.,* 201 (2007) 9491-9496